J. Fluid Mech. (1973), *vol.* 58, *part* 2, *pp.* 403–414
Printed in Great Britain

Turbulent flow with wavy permeable boundaries

By R. T. HO AND L. W. GELHAR
Department of Civil Engineering, Massachusetts Institute of Technology

(Received 14 December 1972)

The effects of a wavy permeable boundary on turbulent flow are investigated theoretically and experimentally, mainly in terms of the pressure distribution along the wavy boundary and the friction factors. A simplified theoretical analysis based on potential flow theory and a linear Darcy equation shows that the perturbations of the flow field have a phase shift relative to the wavy surface and that, owing to this phase shift, there results a net form resistance on the wavy surface. Experiments were conducted in two pipelines with different sizes of granular material lining the inside of the pipe walls. The diameter of the porous conduits varied sinusoidally. The experimental results show that there is a phase shift between the boundary wave form and the pressure distribution and that friction factors increase with Reynolds number even though the flow is within the normal fully rough regime.

1. Introduction

For decades, hydraulic engineers have sought predictions of flow resistance in alluvial channels under various flow conditions (e.g. Vanoni & Brooks 1957; Simons & Richardson 1960; Raudkivi 1967, etc.). The complexity of this phenomenon is largely related to the different types of bed configurations which can occur in alluvial channels under various flow conditions. These bed forms result from the interaction between the turbulent fluid motion of the stream and the alluvial channel bed. Flow turbulence is the major feature of the interaction and it contributes to the sediment motion and the formation of bed forms. Both the mean flow and turbulence in the porous bed may influence the sediment motion, the flow resistance and the turbulence structure of the main flow over it.

Eckert, Diaguila & Donoughe (1955), Yuan & Brogren (1961) and Olsen & Eckert (1966) have investigated turbulent flow over porous walls with air injection or suction through the boundary. Munoz Goma & Gelhar (1968) and Chu & Gelhar (1972) have observed unusually high turbulence levels in pipe flow with porous walls. They also found that the friction factors in the porous pipes increased continuously with Reynolds number even though the flow was within the normal fully rough regime. Lovera & Kennedy (1969) also found friction factors increasing with Reynolds number for flat-bed flows in sand channels. Many studies have dealt with turbulent flow over wavy boundaries, mainly in relation to wind-wave generation and the formation of bed forms in alluvial channels. For turbulent flow over rigid wavy impermeable boundaries, Motzfeld (1937), Hsu (1968) and Hsu & Kennedy (1971) observed a slight phase shift of the wall pressure distributions relative to the sinusoidal wavy surface. Benjamin

(1959) studied analytically the problem of shear flow over wavy impermeable boundaries and predicted a phase shift between the pressure distributions and the boundary wave form. Such phase shifts between the flow properties and the boundary geometry have been found to play an important role in the development of the wavy interfaces in growing wind-generated water waves (Miles 1957), or the formation of various bed forms in alluvial channels (Kennedy 1963).

The objective here is to evaluate the interaction between the mean flow in a wavy permeable boundary and the external flow as reflected in boundary pressure distributions and flow resistance. A theoretical analysis based on potential flow theory and the linear Darcy equation was developed first to indicate some major characteristics of the flow over wavy permeable boundaries. Then experiments were designed according to the information derived from the analysis. The experimental results, including the mean pressure gradient, the friction factor and the wall pressure distributions along the wavy boundary, are presented and discussed.

2. Theoretical analysis

Both two-dimensional and axisymmetric flows are analysed, using potential flow theory and the linear Darcy equation to investigate effects of a wavy permeable boundary on the mean flow over it.

For an initially uniform flow passing over a two-dimensional sinusoidal permeable boundary $y = \eta(x) = a\sin\alpha x$ of small amplitude, there will be some small perturbation in the flow field. The velocity field $\mathbf{V}$ in the main stream ($y \geqslant \eta$) will be

$$\mathbf{V} = (U+u, v) = (U+\partial\phi/\partial x, \partial\phi/\partial y), \tag{1}$$

where U is the undisturbed velocity of the mean flow, u and v are the perturbation velocity components and ϕ is the velocity potential for the perturbed flow field. For the perturbed flow field inside the porous media, based on the linear Darcy equation, the specific discharge is

$$\mathbf{q} = (u', v') = -\frac{k}{\mu}\nabla(p'+\rho g y) = \left(\frac{\partial\phi'}{\partial x}, \frac{\partial\phi'}{\partial y}\right) \tag{2}$$

when expressed in terms of the velocity potential

$$\phi' = -(k/\mu)(p'+\rho g y). \tag{3}$$

Here k is the intrinsic permeability of the porous medium, μ is the viscosity, p' is the pressure, ρ is the fluid density and g is the acceleration due to gravity. Using the continuity equations $\nabla.\mathbf{V} = 0$ and $\nabla.\mathbf{q} = 0$ for an incompressible fluid,

$$\nabla^2\phi = 0 \quad \text{for} \quad y \geqslant \eta, \tag{4}$$

$$\nabla^2\phi' = 0 \quad \text{for} \quad y \leqslant \eta, \tag{5}$$

with the boundary conditions

$$u, v \to 0 \quad \text{as} \quad y \to \infty, \tag{6a}$$

$$u', v' \to 0 \quad \text{as} \quad y \to -\infty, \tag{6b}$$

$$p = p' \quad \text{at} \quad y = \eta, \tag{6c}$$

$$\mathbf{V}.\mathbf{n} = \mathbf{q}.\mathbf{n} \quad \text{at} \quad y = \eta, \quad \mathbf{n} = \nabla(y-\eta). \tag{6d}$$

Here the continuity of pressure and mass flux at the wavy boundary are used.

For small amplitudes $a \ll L$ ($L = 2\pi/\alpha$), the boundary conditions on the wavy boundary $y = \eta$ can be approximated by using Taylor series expansions such that the conditions can, to lowest order in αa, be evaluated at $y = 0$ instead of at $y = \eta$. To lowest order in αa the pressure condition, using the Bernoulli equation for the flow outside the boundary, reduces to

$$\mu\phi'/k = \rho U\,\partial\phi/\partial x \quad \text{at} \quad y = 0 \tag{7a}$$

and the flux condition becomes

$$\frac{\partial\phi}{\partial y} - \frac{\partial\phi'}{\partial y} = U\alpha a\cos\alpha x \quad \text{at} \quad y = 0. \tag{7b}$$

To the lowest order in αa, the solutions are as follows:

$$\phi = -\frac{Ua}{(1+R^2)^{\frac{1}{2}}}\cos(\alpha x - \delta)\,e^{-\alpha y}, \tag{8a}$$

$$p + \rho g y = -\rho U u = -\frac{\rho U^2\alpha a}{(1+R^2)^{\frac{1}{2}}}\sin(\alpha x - \delta)\,e^{-\alpha y}, \tag{8b}$$

$$\phi' = \frac{UaR}{(1+R^2)^{\frac{1}{2}}}\sin(\alpha x - \delta)\,e^{\alpha y}, \tag{9}$$

where $R = U\alpha k/\nu$ is a Reynolds number based on the intrinsic permeability k of the porous media and the wavenumber α, and $\delta = \tan^{-1}R$. The streamline pattern of this flow is shown in figure 1. A kind of separation zone occurs above the porous boundary.

The major features here are that all the $O(\alpha a)$ perturbation quantities have the same phase shift angle δ relative to the boundary wave form and that this phase shift δ depends on the free-stream velocity U, the wavenumber α, the permeability k and the kinematic viscosity ν. If the boundary is impermeable, i.e. $k = 0$, there will be no phase shift in the perturbation quantities, i.e. $\delta = 0$. Owing to this phase shift in the boundary pressure, there will be a net form drag force acting on the wavy boundary. The pressure at the wavy surface $y = \eta$ is, for small αa, approximated by

$$p + \rho g\eta = -\frac{\rho U^2\alpha a}{(1+R^2)^{\frac{1}{2}}}\sin(\alpha x - \delta) \tag{10}$$

and the average form drag force per unit length is

$$\tau_p = \frac{1}{L}\int_0^L p\frac{d\eta}{dx}dx = \frac{\rho U^2(\alpha a)^2}{2(1+R^2)^{\frac{1}{2}}}\sin\delta. \tag{11}$$

The form drag friction factor f'', defined by $\tau_p = \frac{1}{8}f''\rho U^2$, is given by

$$f'' = \frac{4(\alpha a)^2}{(1+R^2)^{\frac{1}{2}}}\sin\delta. \tag{12}$$

The friction factor f'' will increase with the phase shift δ, and δ will increase with the mean free-stream velocity U for a fixed wavy permeable boundary, i.e. αa and k are constants.

For the case of uniform flow through a circular pipe with a sinusoidal permeable boundary $\eta = r_i - a\sin\alpha x$, the formulation is similar to that for the

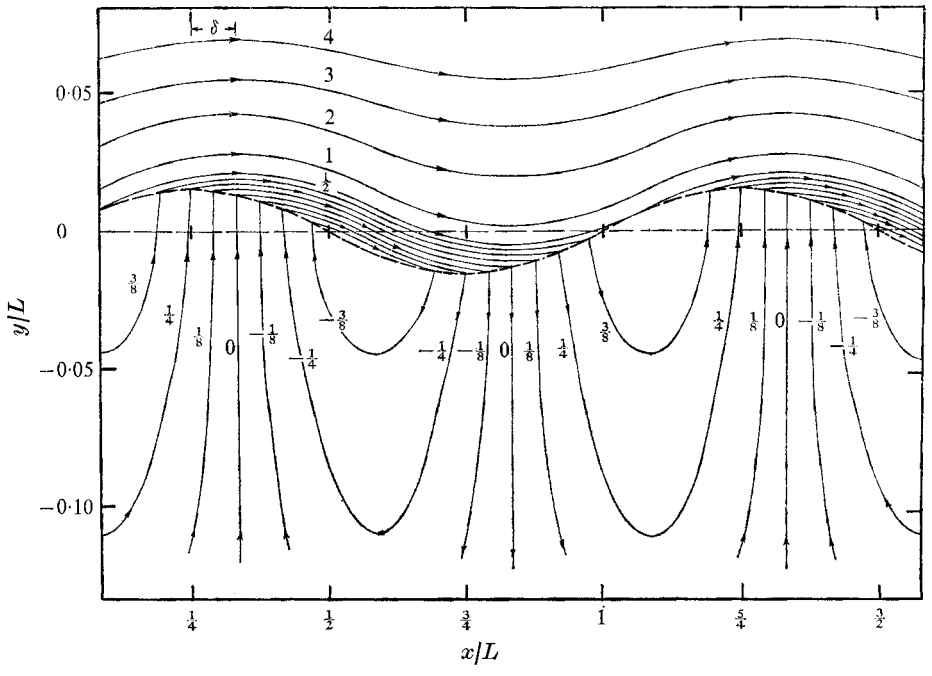

FIGURE 1. Streamline pattern for $\delta = \frac{1}{6}\pi$ and $\alpha a = 0{\cdot}10$ (values of the stream function normalized by Ua are shown).

two-dimensional case. In cylindrical co-ordinates (r, x), the governing equations are

$$\nabla^2\phi = 0 \quad \text{for} \quad \eta \geqslant r \geqslant 0, \tag{13}$$

$$\nabla^2\phi' = 0 \quad \text{for} \quad r_0 \geqslant r \geqslant \eta \tag{14}$$

and the boundary conditions are, with $\alpha a \ll 1$,

$$\partial\phi/\partial r = 0 \quad \text{at} \quad r = 0, \tag{15a}$$

$$\partial\phi'/\partial r = 0 \quad \text{at} \quad r = r_0, \tag{15b}$$

$$\rho U \frac{\partial\phi}{\partial x} = \frac{\mu}{k}\phi', \quad \frac{\partial\phi}{\partial r} - \frac{\partial\phi'}{\partial r} = -U\alpha a \cos\alpha x \quad \text{at} \quad r = r_i, \tag{15c,d}$$

where r_i is the radius to the mean level of the wavy boundary and r_0 is the radius to the solid wall.

The solutions are, for small αa,

$$\phi = -\frac{Ua}{(1+R_1^2)^{\frac{1}{2}}} \frac{I_0(\alpha r)}{I_1(\alpha r_i)} \cos(\alpha x - \delta_1), \tag{16a}$$

$$p_d = -\rho U u = -\frac{\rho U^2 \alpha a}{(1+R_1^2)^{\frac{1}{2}}} \frac{I_0(\alpha r)}{I_1(\alpha r_i)} \sin(\alpha x - \delta_1), \tag{16b}$$

$$\phi' = \frac{UaR_1}{(1+R_1^2)^{\frac{1}{2}}} \frac{K_0(\alpha r)/I_0(\alpha r) + K_1(\alpha r_0)/I_1(\alpha r_0)}{K_1(\alpha r_i)/I_1(\alpha r_i) - K_1(\alpha r_0)/I_1(\alpha r_0)} \frac{I_0(\alpha r)}{I_1(\alpha r_i)} \sin(\alpha x - \delta_1), \tag{17a}$$

$$p_d' = -\frac{\mu}{k}\phi' = -\frac{\rho U^2 \alpha a}{(1+R_1^2)^{\frac{1}{2}}} \frac{K_0(\alpha r)/I_0(\alpha r) + K_1(\alpha r_0)/I_1(\alpha r_0)}{K_0(\alpha r_i)/I_0(\alpha r_i) + K_1(\alpha r_0)/I_1(\alpha r_0)} \frac{I_0(\alpha r)}{I_1(\alpha r_i)} \sin(\alpha x - \delta_1), \tag{17b}$$

Wavy pipe	a (cm)	L (cm)	$\alpha a = 2\pi a/L$	Mean diameter $2r_i$ (cm)	Number of waves	Total length (cm)	Bead size (mm)	Permeability k (cm^2)	$2r_0$ (cm)
1	0·483	30·48	0·10	4·445	9·5	289·6	3·05	$1{\cdot}47 \times 10^{-4}$	7·32
2	0·483	30·48	0·10	4·445	9·5	289·6	1·83	$4{\cdot}41 \times 10^{-5}$	7·32

TABLE 1. Conduit dimensions and media properties

where
$$R_1 = \frac{U\alpha k}{\nu} \frac{K_1(\alpha r_i)/I_1(\alpha r_i) - K_1(\alpha r_0)/I_1(\alpha r_0)}{K_1(\alpha r_0)/I_1(\alpha r_0) + K_0(\alpha r_i)/I_0(\alpha r_i)}, \tag{18a}$$

$$\delta_1 = \tan^{-1} R_1. \tag{18b}$$

The pressure field is expressed in terms of the dynamic pressures p_d and p'_d. I_0, I_1, K_0 and K_1 are modified Bessel functions. The form drag friction factor is

$$f'' = \frac{4(\alpha a)^2}{(1+R_1^2)^{\frac{1}{2}}} \frac{I_0(\alpha r_i)}{I_1(\alpha r_i)} \sin\delta_1. \tag{19}$$

The major features for the axisymmetric case are the same as those for the two-dimensional case. Only the magnitudes of these perturbation quantities differ by certain constant factors depending upon the geometrical parameters. Higher order solutions can be found by a similar method. They have smaller amplitude than the $O(\alpha a)$ solutions, and since they involve only higher harmonics $\sin n\alpha x$ and $\cos n\alpha x$, the higher order perturbed pressure fields do not produce a net form drag on the wavy boundary.

3. Experiments

Two circular conduits, lined with a layer of granular permeable material which varies sinusoidally, were used in these air flow experiments. In the design of the wavy conduits, it was necessary for the maximum amplitude-to-wavelength ratio or αa to be such that no flow separation was produced and that the number of waves was sufficient to generate a quasi-uniform flow. Hsu (1968) and Hsu & Kennedy (1971) reported that, for an impermeable wavy boundary, the flow is free of separation for $a/L < \frac{1}{35}$ and that five wavelengths are sufficient for the establishment of quasi-uniform flow. In this study, $\alpha a = 0{\cdot}10$ ($a/L \cong \frac{1}{63}$) was chosen and both pipelines were 9·5 wavelengths long.

In the selection of porous material, the requirements to be satisfied were that (*a*) the mean flow be in the range of turbulent flow, (*b*) the effects due to the wavy permeable boundaries on the mean flow, in terms of the perturbation variations of the wall pressure, be measurable and (*c*) the velocity inside the porous media be low enough such that linear Darcy equation would be applicable. The permeable conduits were constructed using an axisymmetric internal form of sinusoidal shape which was placed concentrically in a circular pipe. The annular space was then filled with expanded polystyrene beads with an epoxy binder. The conduit dimensions and media properties used in these experiments are shown in table 1. The permeability was measured in a permeameter which

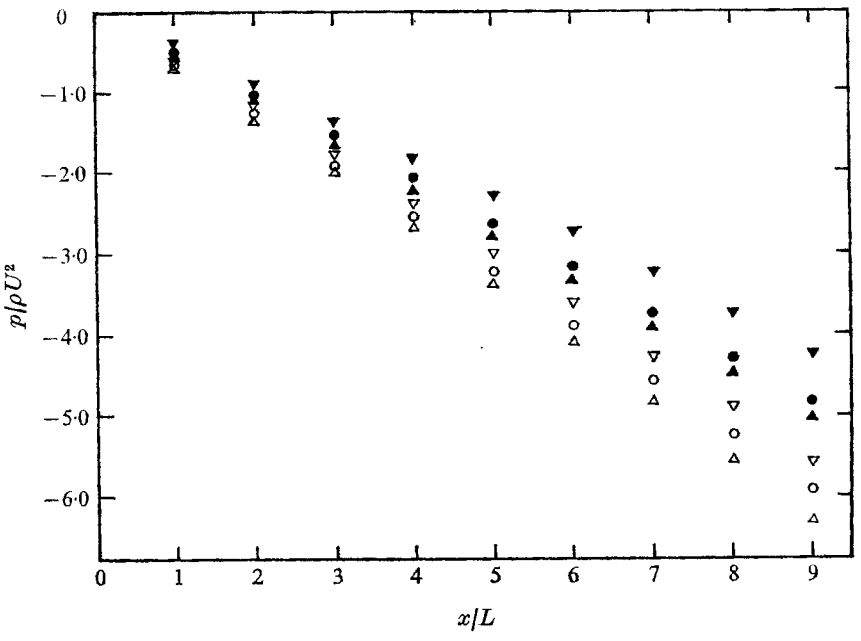

FIGURE 2. Mean pressure distribution. For the first wavy pipe: ▽, $U = 8{\cdot}19$ m/s; ○, $U = 12{\cdot}30$ m/s; △, $U = 24{\cdot}28$ m/s. For the second pipe: ▼, $U = 9{\cdot}47$ m/s; ●, $U = 16{\cdot}09$ m/s; ▲, $U = 31{\cdot}66$ m/s.

consisted of a segment half a wavelength long of the porous conduit with an impermeable inner lining.

For pressure measurement in the test section, consisting of the last wavelength, 19 piezometric openings 1·59 mm in diameter were drilled in the pipe wall per wavelength. The mean pressure gradient was measured from the pressure difference between pairs of piezometric holes one wavelength apart starting from the first section throughout the whole pipeline. The distributions of the wall pressure were determined through the detailed measurements of the relative pressure of every piezometric hole of the test section. The pressure differences were measured with a micromanometer. For the boundary configuration used in these experiments it can be shown, using the solution for flow in the boundary, that the pressure at the surface of the wavy boundary is practically the same as that at the base of the porous layer at the pipe wall.

4. Results

The mean pressure gradients measured in both wavy pipes are shown in figure 2. A constant mean pressure gradient developed for both wavy pipes, thus indicating that the pressure field had reached a quasi-uniform state. From the mean pressure gradient $\overline{dp/dx}$, a gross friction factor f was determined from

$$-\overline{\frac{dp}{dx}} = f\frac{1}{D}\frac{\rho U^2}{2}, \tag{20}$$

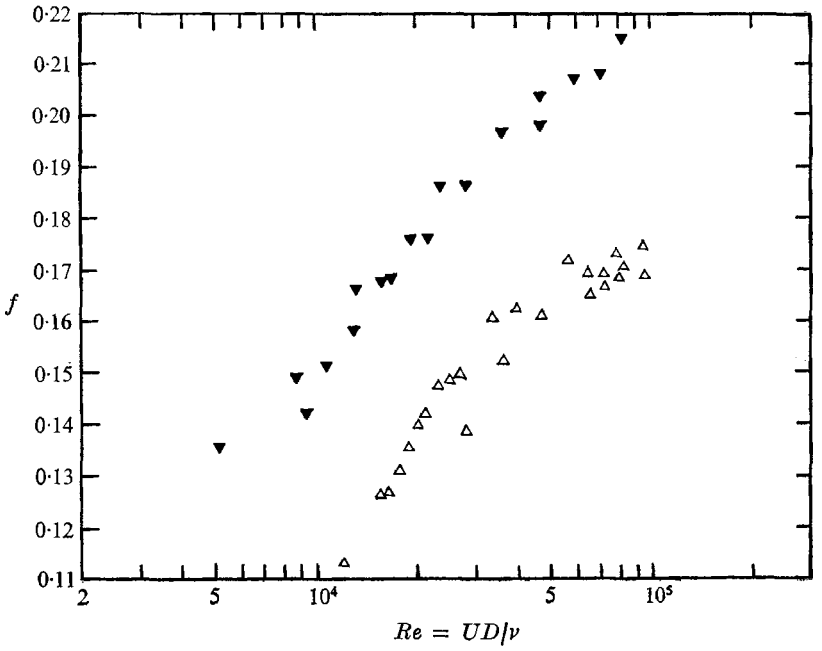

FIGURE 3. Total friction factor f in the porous wavy pipes. ▼, first wavy pipe ($2r_i/\sqrt{k} = 370$); △, second wavy pipe ($2r_i/\sqrt{k} = 670$).

where U is the average velocity in the wavy pipe with a mean diameter D. The results of the friction factor are shown in figure 3. They all indicated a drastic increase of friction factors with Reynolds number. The friction factors in the first wavy pipe, which had a lining of larger beads and higher permeability, were of larger magnitude than those in the second wavy pipe.

The same trends of continuous increase in friction factors with Reynolds number were observed in measurements of turbulent flow over flat porous boundaries by Munoz Goma & Gelhar (1968) and Chu & Gelhar (1972). However, for the present case of turbulent flow over wavy permeable boundaries, the rates of increase of friction factors were much higher than those observed for flat boundaries.

The distributions of the perturbation wall pressure for different mean flow velocities in the wavy pipes are shown in figures 4(*a*)–(*c*). It can be seen that the pressure distributions for all velocities in both pipes do have a certain phase shift relative to the wavy surface as expected from theoretical analysis; however, they all involve complex wave forms.

Since the pressure distributions are all periodic with the same wavelength as the wavy surface, they can be decomposed into a series of Fourier components. The Fourier coefficients were evaluated by using numerical integration methods. Typical results of the first and second harmonic components are shown in figure 4. Only the first harmonic component, which has the same wavelength as the wavy boundary, will contribute an average form drag acting on the wavy surface. All higher harmonic components, being orthogonal to the first harmonic, give no contribution. However, the effects of nonlinear interaction may affect the magnitude of the phase shift and the amplitude of the first harmonic

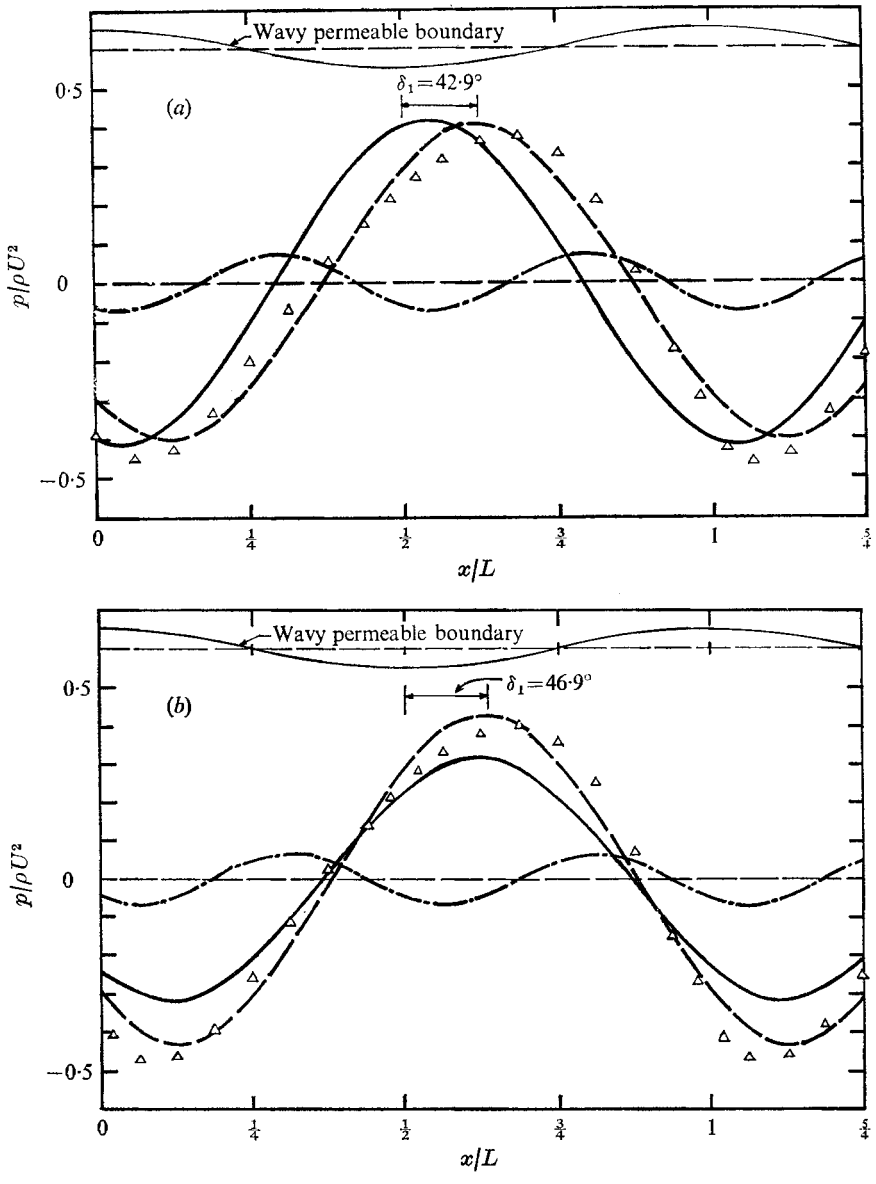

FIGURES 4 (*a*) and (*b*). For legend see facing page.

component and contribute to the form resistance indirectly. Table 2 and figure 4 show the comparison of the measured first harmonic components and theoretical wall pressure distributions predicted by (17*b*). It can be seen that the measured pressure distributions in both wavy pipes have significantly larger phase shifts than the predicted values, especially at the lower velocities. The observed phase shift increases with mean velocity but the amplitude of the measured pressure distribution is practically independent of velocity.

It has been shown in figure 3 that the friction factor f increases with Reynolds number in both wavy pipes. These observations are within the range where it

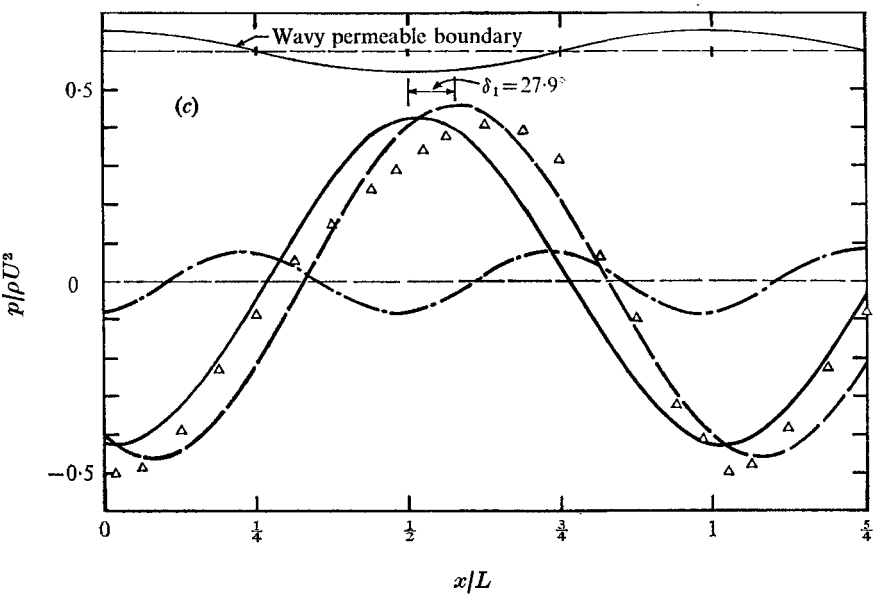

FIGURE 4. First and second harmonic components of the measured wall pressure. △, measured data; — —, first harmonic; — · —, second harmonic; ——, theoretical wall pressure. (*a*) Run 1–3, $U = 8{\cdot}18$ m/s. (*b*) Run 1–8, $U = 28{\cdot}11$ m/s. (*c*) Run 2–1, $U = 9{\cdot}47$ m/s.

Run	Mean velocity U (m/s)	Reynolds number UD/ν	R_1	Measured p (first harmonic) Amplitude	δ_1 (deg)	Theoretical p $p_{max}/\rho U^2$	δ_1 (deg)
			(i) First wavy pipe $k = 1{\cdot}47 \times 10^{-4}$ cm				
1–10	3·19	$9{\cdot}35 \times 10^3$	0·1049	0·4191	30·92	0·4269	5·99
1–11	4·50	$1{\cdot}06 \times 10^4$	0·1480	0·4064	35·51	0·4213	8·42
1–3	8·19	$2{\cdot}40 \times 10^4$	0·2689	0·3988	42·87	0·4144	15·05
1–5	16·00	$4{\cdot}68 \times 10^4$	0·5253	0·4172	46·10	0·3799	27·71
1–9	16·04	$4{\cdot}70 \times 10^4$	0·5267	0·4106	46·30	0·3688	27·78
1–6	20·21	$5{\cdot}92 \times 10^4$	0·6636	0·4273	46·55	0·3576	33·57
1–7	24·28	$7{\cdot}11 \times 10^4$	0·7971	0·4230	47·25	0·3356	38·56
1–8	28·11	$8{\cdot}23 \times 10^4$	0·9228	0·4284	46·92	0·3154	42·70
			(ii) Second wavy pipe $k = 4{\cdot}41 \times 10^{-5}$ cm^2				
2–6	5·37	$1{\cdot}57 \times 10^4$	0·0531	0·4461	21·43	0·4285	3·04
2–1	9·47	$2{\cdot}77 \times 10^4$	0·0938	0·4600	27·93	0·4273	5·36
2–2	12·33	$3{\cdot}61 \times 10^4$	0·1221	0·4231	32·66	0·4262	6·96
2–3	16·09	$4{\cdot}71 \times 10^4$	0·1593	0·4322	34·00	0·4238	9·05
2–5	24·44	$7{\cdot}15 \times 10^4$	0·2420	0·4264	36·70	0·4171	13·60
2–4	31·66	$9{\cdot}27 \times 10^4$	0·3135	0·4152	37·22	0·4095	17·40

D = mean diameter of the wavy pipe = 4·445 cm, ν = kinematic viscosity, R_1 is the parameter defined in (18*a*).

TABLE 2. Comparison of measured and theoretical wall pressure

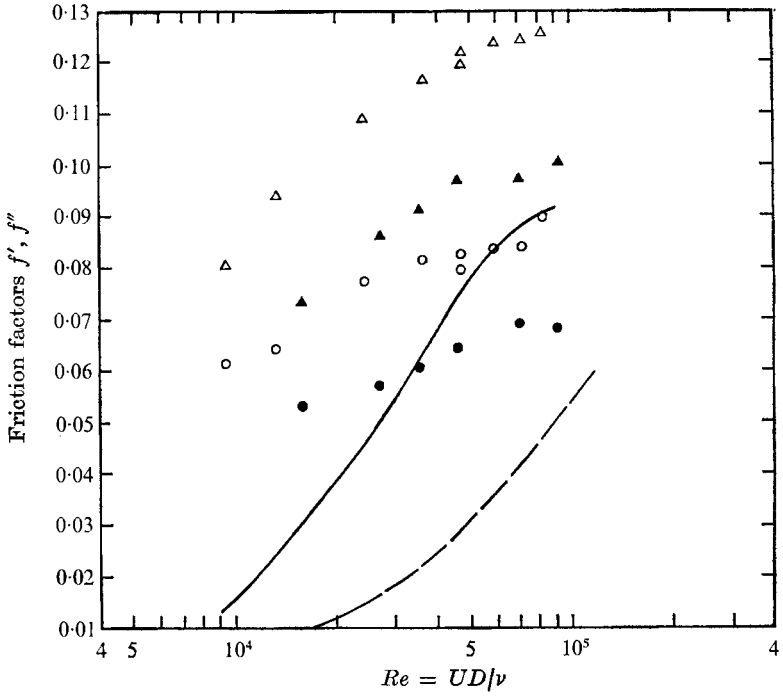

FIGURE 5. Friction factors f' and f'' in the wavy pipes. First pipe: ○, f'; △, f''; ——, predicted f''. Second pipe: ●, f'; ▲, f''; — —, predicted f''.

is usually found that the friction factors are independent of Reynolds number for fully rough flows over impermeable boundaries.

The gross friction factor f can be divided into two parts:

$$f = f' + f'', \tag{21}$$

where f' is associated with the surface resistance due to the flat porous boundary and f'' is due to the form drag resulting from the pressure difference between the front and lee sides of the wavy surface. By definition, f'' can be calculated from the pressure distribution along the wave permeable surface as follows:

$$f'' = 8\frac{\tau_p}{\rho U^2} = \frac{8}{L}\int_0^L \frac{p}{\rho U^2}\frac{d\eta}{dx}dx, \tag{22}$$

and then f' can be found by subtracting f'' from f. The results for f' and f'' for both wavy pipes are shown in figure 5. It can be seen that (*a*) both f' and f'' increase with Reynolds number and the magnitude of f'' is larger than that of f' in both porous wavy pipes, and (*b*) the magnitudes of f' and f'' in the first wavy pipe, which has a larger permeability, are all larger than the corresponding values in the second pipe. Since the amplitude of the measured pressure (see table 2) does not vary much, the form drag friction factor f'' is mainly dependent upon the magnitude of the phase shift. The values of f'' predicted by theoretical analysis are lower than the measured f'' because the predicted phase shifts, based on potential flow theory and the linear Darcy equation, are lower than the measured values.

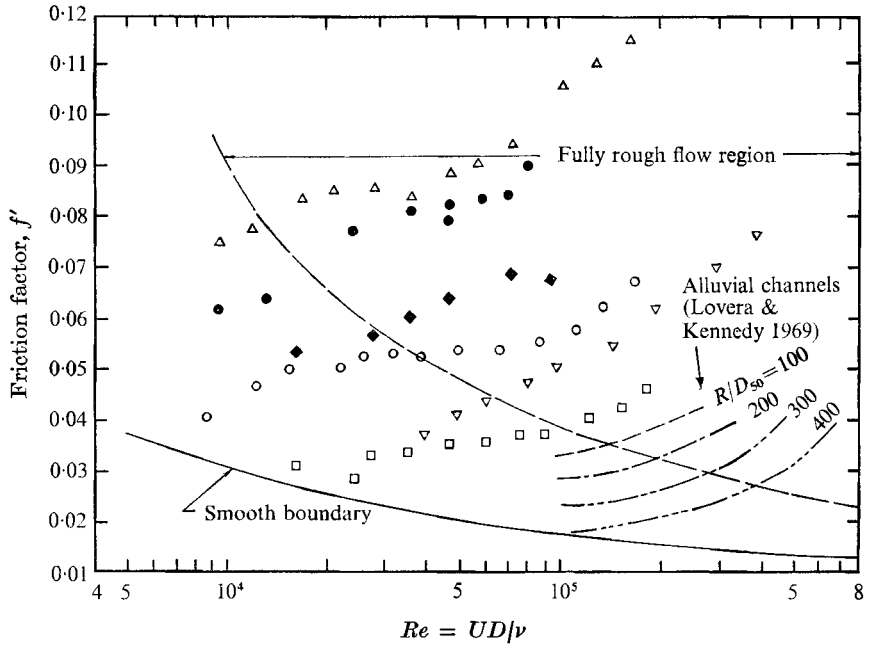

FIGURE 6. Comparison of friction factor f'. (R = hydraulic radius; D_{50} = mean grain size.) Chu & Gelhar (1972), flat boundaries: ○, $2r_i/\sqrt{k} = 48$, granular; □, $2r_i/\sqrt{k} = 960$, granular; △, $2r_i/\sqrt{k} = 230$, porous foam; ▽, $2r_i/\sqrt{k} = 700$, porous foam. Present results, wavy permeable boundaries: ●, $2r_i/\sqrt{k} = 370$; ◆, $2r_i/\sqrt{k} = 670$.

Munoz Goma & Gelhar (1968) and Chu & Gelhar (1972) observed that the friction factor f' for turbulent flow over flat porous boundaries increases continuously with Reynolds number even though the flow is well within the usual fully rough regime. The comparison of the measured f' in this study with those observed by above investigators is shown in figure 6. It is seen that they show similar trends of increase with Reynolds number. Lovera & Kennedy (1969) found that the friction increases continuously with Reynolds number for flat-bed flows in sand channels as shown in figure 6. In contrast, Vanoni & Hwang (1967) reported, from their measurements of open-channel flow over a rigid (and apparently impermeable) sand bed with ripples, that, for a constant flow depth, the bed friction factor is independent of Reynolds number.

5. Discussion

The series of experiments for pipe flow demonstrate the effects of boundary permeability in flow over undular bed forms. The phase shift between the bed form and the pressure distribution increases with increasing boundary permeability. Friction factors are larger for the pipe with larger boundary permeability. The gross friction factor as well as those associated with both form and surface drag increase with increasing Reynolds number. A potential flow analysis of flow over an undular permeable boundary shows trends similar to those observed. The computed amplitude of the pressure perturbation is similar

to that observed but the phase shift between the bed form and the pressure distribution is generally lower than that observed especially at the lower velocities. Predicted form drag friction factors, being primarily dependent on the phase shift, are also lower than those observed.

A primary weakness of this simple potential flow model is the omission of shear in the mean flow. An explicit evaluation of this shear effect is not possible but some estimates using a typical turbulent velocity profile in the analysis by Benjamin (1959) for an impermeable wavy boundary indicate that phase shifts of the magnitude of the observed differences are possible. Nonlinear resistance effects in the porous boundary may also have affected the results for the larger permeability at high velocities.

In general, both the analysis and the experiments show that the mean flow within a wavy permeable boundary can have a significant influence on the external flow field and hence the form resistance. These boundary permeability effects should be evaluated in analyses of alluvial channel bed forms.

This research was sponsored by the National Science Foundation under Grant No. GK31774X.

REFERENCES

BENJAMIN, T. B. 1959 Shearing flow over a wavy boundary. *J. Fluid Mech.* **6**, 161–205.

CHU, Y. S. & GELHAR, L. W. 1972 Turbulent pipe flow with granular permeable boundaries. *Ralph M. Parsons Lab. for Water Resources & Hydrodynamics, M.I.T. Rep.* no. 148.

ECKERT, E. R. G., DIAGUILA, A. J. & DONOUGHE, P. L. 1955 Experiments on turbulent flow through channels having porous rough surfaces with and without air injection. *N.A.C.A. Tech. Note*, no. 3339.

HSU, S. T. 1968 Turbulent flow in wavy pipes. Ph.D. thesis, University of Iowa.

HSU, S. T. & KENNEDY, F. F. 1971 Turbulent flow in wavy pipes. *J. Fluid Mech.* **47**, 481–502.

KENNEDY, J. F. 1963 The mechanics of dunes and antidunes in erodible-bed channels. *J. Fluid Mech.* **16**, 521–44.

LOVERA, F. & KENNEDY, J. F. 1969 Friction factors for flat bed flows in sand channels. *J. Hydraul. Div. A.S.C.E.* **95**, 1227–34.

MILES, J. W. 1957 On the generation of surface waves by shear flows. *J. Fluid Mech.* **3**, 185–204.

MOTZFELD, H. 1937 Die Turbulente Strömung an Welligen Wanden. *Z. angew. Math. Mech.* **17**, 193–212.

MUNOZ GOMA, R. J. & GELHAR, L. W. 1968 Turbulent pipe flow with rough and porous walls. *Hydrodyn. Lab., Dept. Civil Engng, M.I.T. Rep.* no. 109.

OLSEN, R. M. & ECKERT, E. R. G. 1966 Experimental studies of turbulent flow in a porous circular tube with uniform fluid injection through the tube wall. *Trans. A.S.M.E., J. Appl. Mech.* E **33**, 7–17.

RAUDKIVI, A. J. 1967 Analysis of resistance in fluvial channels. *J. Hydraul. Div. A.S.C.E.*, no. HY5, 78–84.

SIMONS, D. G. & RICHARDSON, E. V. 1960 Resistance to flow in alluvial channels. *J. Hydraul. Div. A.S.C.E.*, no. HY 5, 73–99. (See also 1962 *A.S.C.E.* **127**, 927–54.)

VANONI, V. A. & BROOKS, N. H. 1957 Laboratory studies of the roughness and suspended load of alluvial streams. *Cal. Inst. Tech. Sedimentation Lab. Rep.* no. E-68.

VANONI, V. A. & HWANG, L. S. 1967 Relation between bed forms and friction in streams. *J. Hydraul. Div. A.S.C.E.* no. HY 3, 121–44.

YUAN, S. W. & BROGREN, E. W. 1961 Turbulent flow in a circular pipe with porous wall. *Phys. Fluids*, **4**, 368–72.